Physical Chemistry Chemical Physics

ARTICLE

Steering Protein Adsorption at Charged Surfaces: Electric Fields and Ionic Screening

Received 00th January 20xx,
Accepted 00th January 20xx

DOI: 10.1039/x0xx00000x

www.rsc.org/

Paul A. Mulheran[a]†, David J. Connell[a] and Karina Kubiak-Ossowska[a]

Protein adsorption at charged surfaces is a common process in the development of functional technological devices. Accurately reproducing the environment above the surface in simulations is essential for understanding how the adsorption process can be influenced and utilised. Here we present a simulation strategy that includes the electric field above the charged surface as well as the screening ions in solution, using standard molecular dynamics tools. With this approach we investigate the adsorption of Hen Egg White Lysozyme (HEWL) onto a model charged silica surface. We find that the screening effects of the ions slow down the adsorption process, giving the protein more time to find its optimal orientation as it adsorbs. Furthermore, we find that the concentrated ionic region directly above the surface helps to stabilise the protein structure in its adsorbed state. Together these effects imply that the adsorbed HEWL might retain its biological activity, with its active site exposed to solution rather than to the surface. Furthermore, this work shows how the steering effects of the electric field, coupled to the ionic screening, might be used to develop general strategies for surface functionalization through protein adsorption for technological applications.

Introduction

Protein adsorption at materials surfaces is a crucial feature of many new biotechnological applications, and has been the focus of much recent research[1-8]. Key questions that still need to be addressed concern not only the extent of protein adsorption, i.e. whether complete surface coverage or even multilayer coverage is achieved, but also the strength of the adhesion to the surface and the functionality of the adsorbed protein[9-14]. These factors directly the affect the utility of the adsorbed proteins for functionalization of surfaces to induce biocompatibility, create antibacterial coatings, or yield novel nanoparticulate drug delivery systems[1].

Modelling has played a major role in advancing our understanding of the adsorption process, since in principle it can reveal molecular-scale insight that is not available experimentally. Well-designed simulations can show not only how proteins adsorb to different surfaces, but also provide understanding of what the driving forces are and how they can be controlled through surface chemistry, and how bio-activity can be preserved by retaining the protein secondary and tertiary structures. There is growing consensus that the orientation of the protein at the surface is paramount, and that this depends on the surface chemistry[11-15]. Of particular note is the idea that electric fields above charged surfaces will play a crucial role in steering the protein during adsorption, and so determine protein orientation once adsorbed[14-16]. Provided that any unfolding induced by interactions with the surface are of limited extent, this provides the means to engineer surface functionalization through controlled protein adsorption[12].

Fully atomistic Molecular Dynamics (MD) has proven to be a valuable modelling strategy, since it can address the 100 ns timescale necessary for the initial protein adsorption process with the necessary system size of ~10^5 atoms required to represent the surface, water, ions and protein[15,16]. Various open source simulation packages exist for this type of simulation, where use can be made of potential sets refined for protein systems, and many insightful studies have been completed. Hen Egg White Lysozyme (HEWL) has extensively been used as a model protein[17-26], since it has anti-bacterial properties which might be preserved when adsorbed to a surface in the correct orientation. HEWL is a hard globular protein of modest size, making it ideal for simulation studies[27-34]. Previous work has considered how it is adsorbed at various surfaces, with the conclusion that negatively charged surfaces, such as mica or silica at physiological conditions, will be best at orienting the protein so that its active site is presented to solution[27-30].

Given the importance of the electric fields at the charged surfaces, it is necessary to consider how the MD simulations can best replicate the environment experienced by the protein as it adsorbs. In recent work we have included electric fields in standard

[a] Department of Chemical and Process Engineering, University of Strathclyde, James Weir Building, 75 Montrose Street, Glasgow G1 1XJ, United Kingdom
† Corresponding author, e-mail: paul.mulheran@strath.ac.uk

Electronic Supplementary Information (ESI) available: The movies showing the trajectories discussed in the manuscript.

simulation methodology by employing silica surface models with intrinsic dipole moments[15,35]. However, we had not until now fully included the effects of ionic screening at the surface. It is the purpose of this paper to do this, and to explore the impact this has on the HEWL adsorption at the model surface. Of crucial importance, we aim to understand whether:

- ionic screening of the charged surface changes the adsorption of the protein or its adsorption pathway;
- the high concentration of ions above a charged surface impacts the structure of the protein in its adsorbed state;
- the electric field and screening effects can be used to enhance our ability to create stable, functional proteins adsorbed to materials with technological potential.

In the following Section we will describe how we set up the simulations to capture the effects of electric field and ionic screening, and the simulation methodology we then employ. In Section 3 we present results from our HEWL adsorption simulations, and the discussion will draw out the comparisons to simulations without full ionic screening. In the final section, we will draw general conclusions that are relevant to the modelling of protein adsorption at charged surfaces.

Methodology

Oxide surfaces such as silica are known to possess a net negative charge at physiological pH. Whilst the detailed structure at the surface might be difficult to characterise, it is believed that the surface will expose hydroxyl and under-coordinated, terminal oxygen species to the solution[36], which are responsible for the net negative charge. Simulations of protein adsorption to these surfaces needs to capture not only the chemistry of these species at the surface, but also the long-range electric field they create in the solution above the surface, which as we have discussed above can play a key role in determining protein orientation as it adsorbs. A key challenge for us is to capture these physical effects in our protein adsorption simulations.

The approach we adopt is illustrated in Figure 1, where we show schematically the electric field surrounding a negatively charged nanoparticle in solution. These nanoparticles are usually ~200nm size range (e.g. silica nanoparticles used for drug delivery[36]), and often much larger than the protein under consideration, so it is reasonable to model adsorption onto a flat surface. This surface needs to expose the relevant species to solution whilst creating the electric field required. In previous work with silica[15,35], we have employed an alpha-crystabolite {11-1} model employed by other groups[36]. However, we consider a stoichiometric slab of the material which has been cut to create a dipole moment in the direction perpendicular to the largest slab surface, with under-coordinated negatively charged oxygen (siloxide groups) at the top surface and under-coordinated positively charged silicon on the bottom. When used in simulations with three-dimensional periodicity and the Ewald summation for electrostatic calculations, as we do here, this creates the desired electric field across the water space of the simulation cell as illustrated in Figure 1. In our simulations, the silica ions are frozen in place to maintain the electric field above the surface; using rigid surface model is a common simulation strategy[37].

This allows us to simulate the adsorption of a protein onto the model negatively charged silica surface. We note that the opposite silicon-rich surface is an artificial construction which does not represent a physically acceptable model surface, so that we are only interested in adsorption to the siloxide-rich surface model. The strength of the electric field is determined by the net dipole moment across the slab and the relative size of the water space to the slab thickness. In the systems used here and in other work, the electric field is measured to be $0.2\ V/\text{Å}$, which is reasonable given the experimentally observed charge density on large silica nanoparticles at pH7[36].

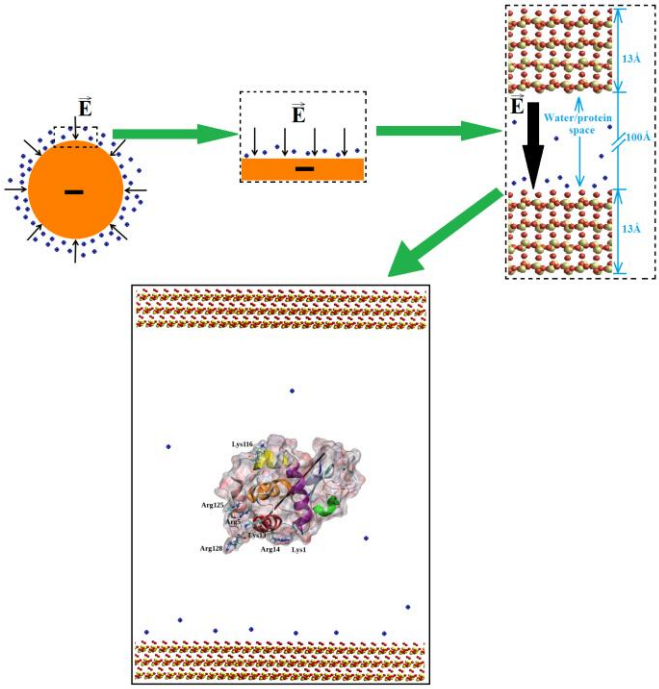

Figure 1. Illustration of the simulation concept. On the left, a negatively charged nanoparticle in solution has an associated electric field screened by the counter ions of the solution. In the middle, we model a portion of the nanoparticle surface as a flat charged surface with a perpendicular electric field. On the right, we create a suitable electric field in a standard material slab model with periodic boundary conditions. Below, we simulate protein adsorption in this system.

As Figure 1 also illustrates, in this work we are interested in the effects of ionic screening on the protein adsorption process. When ions are introduced to the simulation cell, the positive ones are drawn to the negative O-rich surface and the negative ones to the Si-rich surface. In the simulations presented here, the slab size (86Å x 80Å x 13Å) is such that 88 ions of each type will perfectly screen the electric field by removing the dipole moment in the system. If fewer ions are used, we will have incomplete screening, and if more are used we will create a bulk ionic environment in the middle of the water space, which is then representative of the environment above the surface in experiments.

In this paper we consider adsorption simulations with N1 = 1, N2 = 49, and N3 = 182 Na^+ ions in the simulation, with the compensating number of Cl- ions (e.g. N1+9, etc) and a single HEWL protein that has charge +8e at pH7. These simulations are labelled SiO_2_N1a, SiO_2_N1b (a separate version with the same number of Na+ ions) SiO_2_N2 and SiO_2_N3. Full details of our simulation protocol can be found in recent publications[15,35]. In brief, we use NAMD2.6[38] with periodic boundary conditions, the TIP3P water model, the CHARMM27 force-field with a 12Å cut-off for short-range potentials and the Smooth Particle Mesh Ewald Summation

for the electrostatics[39]. Due to the screening effect of the ions, we do not apply any dipole correction to the Ewald summation. There is some debate about the accuracy of CHARMM27 for surface layer effects, however it is a good choice for protein systems[40].

VMD was employed to analyse results[41]. The HEWL structure was downloaded from 1iee.pdb[42] and the four disulphide bridges were retained. The ions were introduced to the simulation box with a single HEWL followed by the SiO_2 surface and then the water. The system minimisation was performed in two steps: first water and ions only are allowed to move, and then water, ions and the protein can relax. The next step was 30ps heating of the entire system to the desired 300K temperature, followed by 270ps equilibration at constant temperature. Finally the production simulations were performed for 100ns with a time-step of 1fs, employing the SHAKE algorithm and periodic boundary conditions. The electrostatic field drove the Na^+ and Cl^- ions towards the negative and positive surfaces during the early stages of the simulations, being apparent during the minimisation period. The ionic screening of the surface was completed within the first few ns of the production trajectories. In the case of the SiO_2_N2 and SiO_2_N3 simulations some ions remained in the bulk water, so that ion exchange was possible.

Results and Discussion

Adsorption Trajectories

In Figure 2 we show protein structures from HEWL adsorption trajectories with the various ion numbers in the simulations. In each case, the protein starts above the negatively charged siloxide-rich SiO_2 surface with a minimum separation of 28Å. During the trajectories the protein adsorbs to the surface adopting commonly observed orientations described elsewhere, namely "side on" and "between" which refer to the long-axis orientation of the protein in relation to the surface plane. In low ionic strength systems, SiO_2_N1a and SiO_2_N1b, where there is virtually no screening of the electric field, we have previously reported that the protein adsorbs within ~4ns[15]. During the first 1ns of the trajectory, the protein rotates and moves towards the surface. This aligns the HEWL dipole moment and presents the N,C-terminal face to the surface. The first contacts with the surface are usually made by the positively charged residues Arg128 (close to the N-terminus) and Lys1, and subsequently further anchoring interactions with the surface are made by available Arg and Lys residues amongst others[15]. We find two possible adsorption orientations due to the flexibility of the protein surface. However, as we explain below, much of the secondary and all the tertiary structure of the HEWL is preserved in these interactions with the model silica surface, and the active cleft of the enzyme is left exposed to solution.

During the preparation stage (potential energy minimisation, heating and equilibration) of the trajectory SiO_2_N2, the Na^+ ions migrate to towards the model negatively charged silica surface whilst the Cl^- migrate to the image surface, creating ion layers ~6Å away from the surfaces with thickness ~4Å. The layers are not very dense and do not greatly disrupt the surface water layers. The protein also translates towards the surface, reducing the Arg128 – surface distance to 17Å.

During the production trajectory of SiO_2_N2 (see movie SiO_2_N2.avi), the initial configuration is maintained for ~5.2ns after which the protein then starts to move towards the surface; the Arg128 and Arg14 side chains are noticeably oriented towards the surface. After a further 0.8ns (e.g 6ns of the trajectory) the Arg128 – surface distance reaches the value ~9Å (e.g. top of the ion layer) and it remains here for another 2ns. At ~8ns, Arg128 starts to penetrate through the ion layer and at ~8.5ns reaches the bottom of the ion layer with a distance to the surface of 6Å. Subsequently, the entire protein is attracted to the surface, and by ~9ns the protein can be considered to be in its initial adsorption stage. Then, without desorbing, the Arg128 side chain changes its orientation from perpendicular to parallel with respect to the surface plane, and the entire protein moves towards the surface. This movement appears to be easier because the ion layer (and the electric field) is already perturbed. The next residues which almost pass the ion layer, without success, at ~10.4ns are Lys1 and Glu7. However at ~12.6ns Arg125 does adsorb with its side chain oriented parallel to the surface. A third anchor adsorption (Arg5) at 18.5ns does not yet complete the initial adsorption stage; the protein slowly rotates on the surface to facilitate Lys33 and Arg114 adsorption (both at 23.7ns and with side chains initially perpendicular to the surface). The HEWL reaches its stable adsorption stage at 24ns. The protein orientation on the surface is "between" (the long protein axis angle is 30^o to the surface plane while the dipole moment angle is 60^o) and this does not change in the remainder of the trajectory. The only notable events after this time are the side chain reorientations to be parallel with the surface, which are completed by ~97ns.

During the preparation stage of the highest ionic strength trajectory SiO_2_N3, we again see the creation of the 4Å thick ionic layers close to the model silica surface and the image. However, as is apparent in Figure 2, in this case there are also many ions in the bulk water/protein space. This impacts the screening of the electric field, allowing ion exchanges into and out of the ion layers at a rate of ~75 ions per ns in this trajectory. The ion exchanges do not disrupt the surface water layers, but provide fluctuations in the screening of the electric field across the simulation cell.

During the production trajectory (see movie SiO_2_N3.avi), the protein does not feel the surface at first and so diffuses freely in the bulk, reaching a "side-on" orientation with protein long axis and dipole moment parallel to the surface plane. However, due to the local field fluctuations caused by the ionic motion, at ~7.8ns the protein moves towards the surface and the minimal distance to the surface starts to fluctuate at ~20Å. From ~14ns the Arg128 side chain is exposed to the solvent and oriented towards the surface. At ~24ns the minimal distance between protein and surface is 15Å and Arg128 clearly starts to act as an anchor, and 2ns later its side chain reaches the top of the ion layer (distance to the surface 10Å) for the first time. However, due to its adverse orientation, the electric field repels the protein away from the surface at this stage.

Further local fluctuations again facilitate protein translation and at ~30.9ns the Arg128 side chain again reaches the top of the ion layer, this time starting to pass through it. Simultaneously the entire protein is attracted to the surface and it also rotates and by 31ns the dipole moment is directed towards the surface. At ~34.1ns the Arg128 successfully adsorbs with its side chain perpendicular to the surface. The protein body continues to move closer to the surface and to rotate, resulting in a "side-on" orientation (the long protein axis parallel to the silica surface) by ~70ns with further residue adsorption completing the adsorption by ~ 75ns.

Physical Chemistry Chemical Physics

ARTICLE

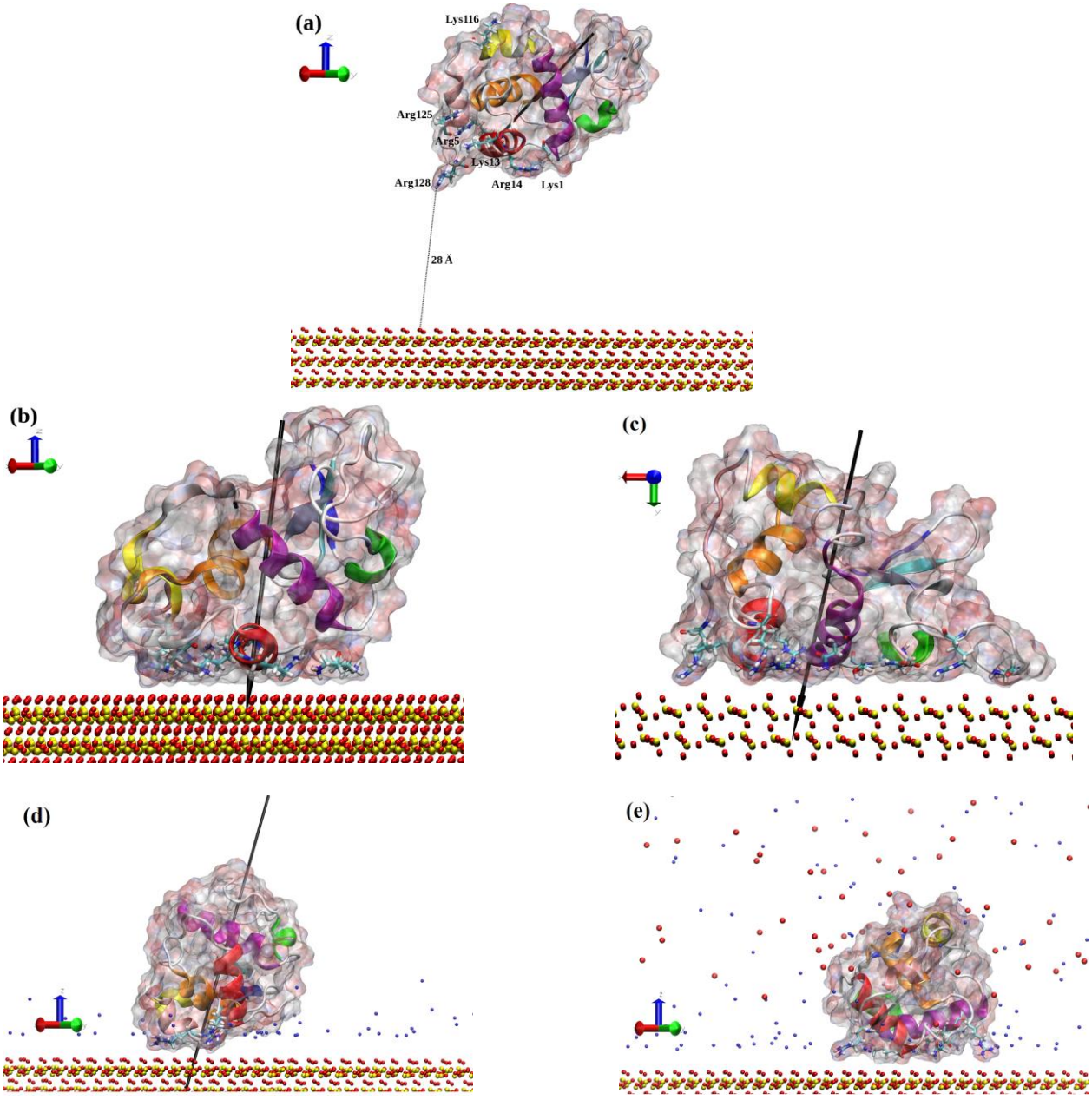

Figure 2. Adsorption simulations of HEWL onto model silica: (a) starting configuration; (b) "between" without screening ions (SiO_2_N1a); (c) "side-on" without screening ions (SiO_2_N1b); (d) "between" at lower ionic screening (SiO_2_N2); (e) "side-on" at highest ionic screening (SiO_2_N3). The needle in each figure shows the dipole moment of the protein.

In comparison with the adsorption trajectories SiO_2_N1a and SiO_2_N1b, where adsorption is complete by ~4ns, we see that the higher ionic concentration slows down the adsorption process without substantially changing the key aspects of the process, namely the preferred orientations of "between" and "side-on" (rather than "end-on") and the key role played by Arg128 in dictating the adsorption process. In the following we will quantify this slower kinetics whilst considering in more detail the behaviour of the screening ions.

Protein Mobility

We monitor the protein mobility on the surface through its centre-of-mass (COM) position over time. Figure 3 shows the COM motion in the low-screening adsorption trajectories SiO_2_N1a and SiO_2_N1b at the model negatively charged silica surface together with trajectories SiO_2_N2 and SiO_2_N3 in higher ionic strength. In these plots, the red lines indicate the period where the protein moves through the solution without contacting the surface. It is clear that the duration of this motion is extended in higher ionic strength screening, lasting 10-30 times longer than the cases without substantial screening of the surface electric field. This means that the protein diffuses more freely in a bulk-solvent environment in these latter simulations, and the longer adsorption timescale provides more opportunity for the protein to find a favourable orientation as it approaches the surface. Nevertheless, the rotation of the protein in the stronger, unscreened electric fields is rapid enough so that adsorption simulations can still be representative of the adsorption process, provided the protein starts far enough above the surface to allow the rotation to be completed before making contact with the surface.

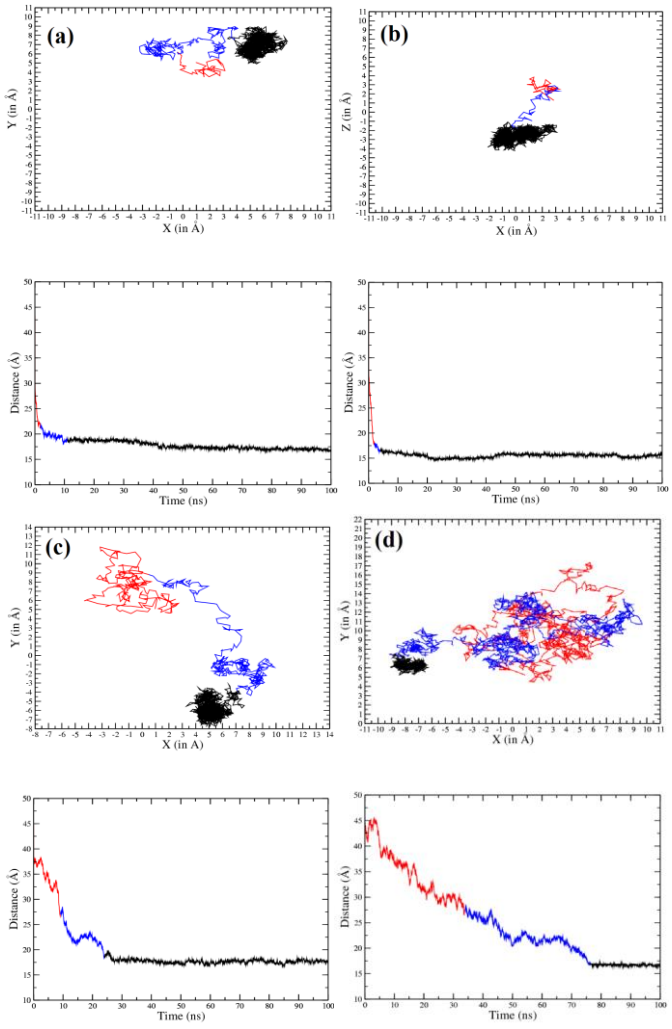

Figure 3. HEWL centre of mass (COM) diffusion. (a) Low ionicity "between" (SiO_2_N1a) and (b) low ionicity "side-on" (SiO_2_N1b); (c) low (SiO_2_N2) and (d) high ionic screening (SiO_2_N3) adsorption trajectories. The top plots show plan views of the diffusion across the plane of the surface and the bottom plots show changes in time of the COM distance perpendicular to the surface. The red part of the plot indicates diffusion before adsorption (stage 1), the blue part indicates diffusion during the initial adsorption state (stage 2) and the black part indicates the diffusion during the stable adsorption state (stage 3).

The blue sections of the plots in Figure 3 show the COM motion when residues are interacting with the surface through extended side-chains. In this phase, the COM continues to move towards the model siloxide surface whilst diffusing across the surface; this motion is due (in part) to the flexibility of the extended side-chains of the anchoring residues. Again it is clear that the higher ionic screening extends the duration of this phase of the adsorption, and a wider exploration of the configuration space is achieved.

The final adsorption stage is shown as the black traces in Figure 3. In all cases, we see that the protein COM becomes well adhered to the surface, maintaining a fairly consistent separation from it ~25Å due to the protein's size. This shows that the protein retains its hardness, so that whilst structural changes do occur at the interface between the siloxide surface and the protein, these are localised in extent and the adsorbed protein retains most of its secondary and tertiary structure. This will be examined further below. Once the adsorption is complete, we do not observe any long-range diffusion of the protein across the surface in our trajectories; this motion requires much longer timescales due to the size of the energy barriers that need to be overcome for surface diffusion[32].

Ion Concentration Fluctuations and the Protein Response

In Fig. 4 plots of the cumulative number of Na^+ ions (i.e. the number within a distance z of the surface) in the higher ionic strength trajectories are shown. Here z is the perpendicular distance above the negative silica surface which is located at z=0. The curves are displayed at different times into the production simulations which started at t=0. The results are taken from the adsorption simulations, and no systematic influence of the protein adsorption on the cumulative ion numbers is apparent. Indeed, as can be seen in the movies, there does not seem to be any synergistic interaction between the protein, the surface and the ions.

The highest ionic strength solution trajectory (SiO_2_N3) results are displayed in the upper plot, which also shows the number of ions (88) for which the electric field due to the charged surface is completely screened. As can be seen, the height above the surface at which complete screening occurs fluctuates between z≈25Å and z≈40Å, due to the thermal motion of the screening ions. For z>40Å, the cumulative ion number follows a straight line trend as expected, producing a bulk-solution environment in the middle of the simulation cell with a Na^+ concentration ~0.27 M (note that the Debye screening length for this concentration is ~6Å). This means that if the protein is greater than ~40Å above the surface it feels no electric field and, as discussed above, it indeed appears that the HEWL diffuses freely when a long way from the surface. However, when the protein approaches closer than ~40Å to the surface, the protein starts to be influenced by the fluctuating electric field. Closer still (z < 25Å), and the protein feels a consistent electric field and starts to align its dipole with it. An alternative view on the strength of the electric field could be obtained from the electrostatic potential[43], although again the fluctuating nature of screening is well presented by these cumulative ion distributions.

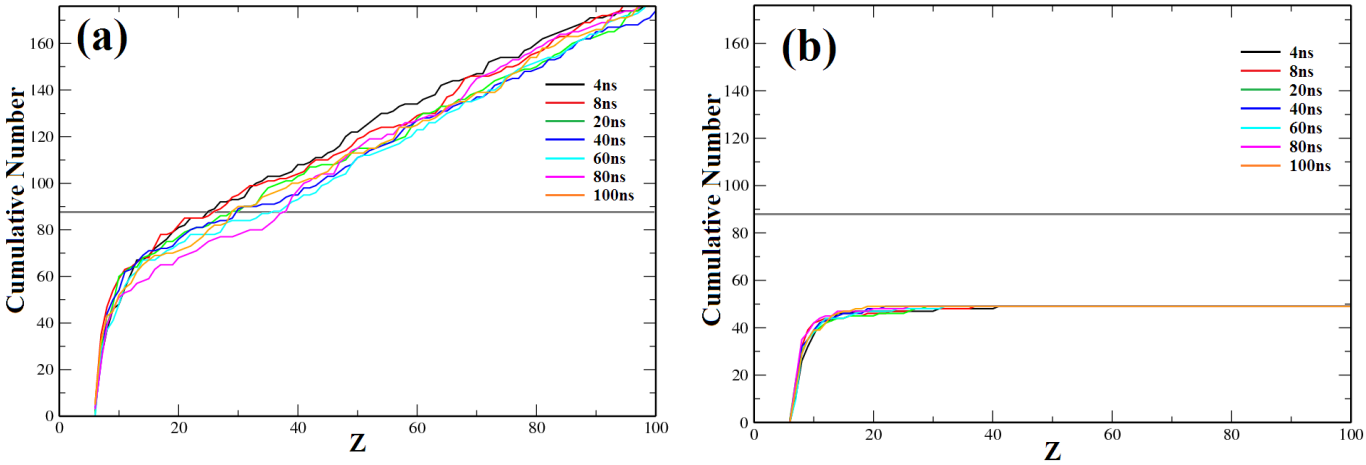

Figure 4. The cumulative distribution of Na+ ions above the negative silica surfaces at different times during the trajectories for (a) high (SiO_2_N3) and (b) low (SiO_2_N2) ionic screening.

In contrast, the Na^+ cumulative plots for the lower ionic strength trajectory SiO_2_N2 show that the screening is incomplete and that the electric field felt by the protein is more stable, with a lower degree of fluctuation and a more tightly-bound layer of ions at the surface. This contrast is apparent in Figs. 2d and 2e, as well as in the movies provided in the Supplementary Information.

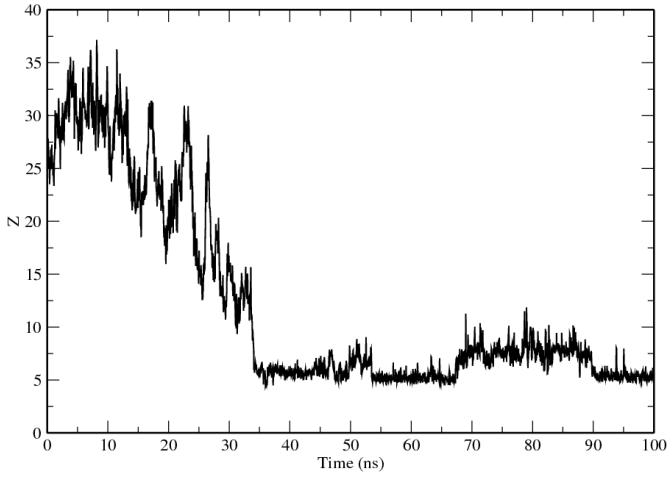

Figure 5. The z-coordinate in Å of the Arg 128 Cz atom as a function of time in the high ionic screening (SiO_2_N3) trajectory.

In Fig. 5 the z-coordinate of the Arg128 Cz atom is plotted as a function of time for the highest ionic strength trajectory, SiO_2_N3. Contrasting this to the centre-of-mass plot shown in Fig. 3d, we see that the side-chain of Arg128 fluctuates in position a lot more than the protein as a whole. Since the guanidinium end-group is positively charged, it responds to fluctuations in the electric field above the negatively charged silica surface as the screening ion density fluctuates. In the SiO_2_N3 trajectory, the Ag128 side-chain extends from the HEWL surface towards the silica, and then retracts as the screening becomes more efficient and the electric field diminishes. This extension and contraction occurs several times in the trajectory. Once the HEWL is closer to the silica surface and exposed to a more consistent electric field, the Arg128 side chain retains its extended conformation and moves steadily towards the silica surface. In this conformation, it is able to penetrate the water layer above the surface to interact directly with the silica species at ~36ns. Thereafter, Arg128 retains a strong interaction with the silica, even while the rest of the HEWL rotates to increase the number of contacts, and eventually helps to anchor the protein as described above. This understanding of the crucial role Arg128 plays in the HEWL adsorption process has been described elsewhere[15,31-32], however we can now add to this picture the role that the electric field fluctuations, caused by the diffusing screening ions, plays in guiding the interactions with the surface and slowing the whole adsorption process.

HEWL Structural Changes Upon Adsorption

Structural changes in the adsorption trajectories can be analysed with the RMSD and RMSF plots shown in Fig. 6. The range of conformational changes strongly depends on the trajectory. As Fig. 6a shows, the trajectories with higher ionic strength, and hence partial or complete screening of the surface, show much lower RMSD values than those at low ionic strength. Structural changes in the higher ionic strength trajectories tend to be limited to the loop regions, as shown in the RMSF plots in Fig 6b. Key secondary structural elements, including the long α-helices A,B,C and D, show much lower levels of fluctuation in their adsorbed state in the higher ionic strength solutions than they do in the absence of the surface screening ions (see previous papers for more discussion of the fluctuation behaviour in these systems[28,30]). This suggests that the ions above the charged surface are playing a role in stabilising the adsorbed protein, in the sense of keeping its structural elements intact[43].

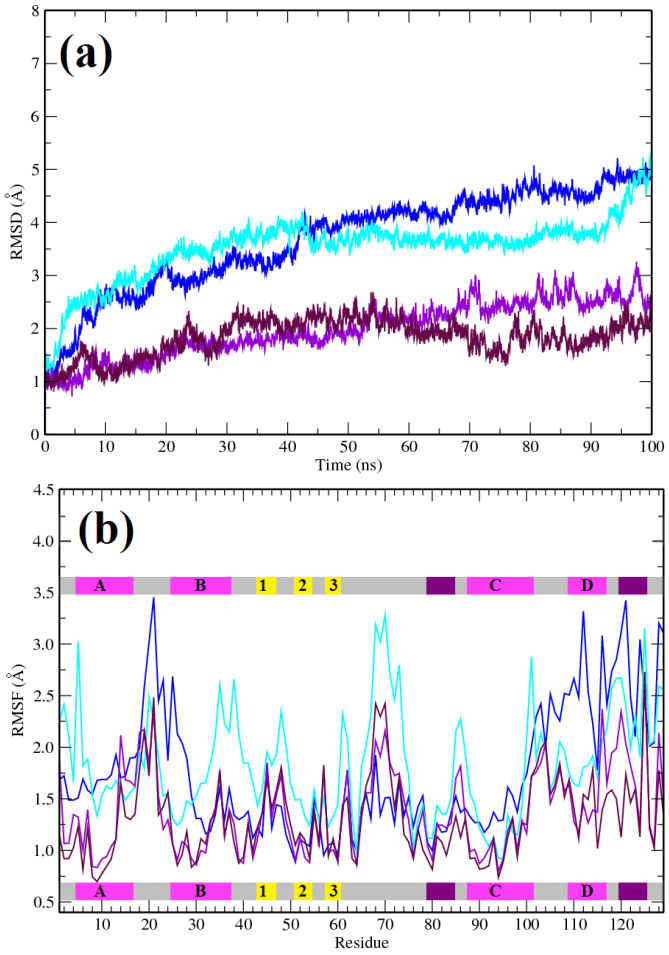

Figure 6. RMSD (a) and RMSF (b) plots calculated with respect to the initial HEWL structure during trajectories SiO_2_N1a (blue) and SiO_2_N1b (cyan) without screening ions, and SiO_2_N2 (purple) and SiO_2_N3 (brown) with screening ions. The colour ribbon at the RMSF indicates secondary structure in the initial HEWL: loops are shown in grey, β structures in yellow, α-helices in pink and α-helices 3_{10} in purple. For clarity β bridges and turns in loops regions are not shown. The main secondary structure elements are annotated. The preparation period (minimisation, heating and equilibration) is omitted.

This structural stabilisation indicates that the protein might well retain its biological activity when adsorbed to the surface, the active site is exposed to the solvent, although further work is required to confirm this suggestion. Real surfaces will have screening ions present, so it is certainly worth noting that the adsorption trajectories without substantial ionic screening appear to over-estimate structural changes upon adsorption.

Conclusions

We have developed a methodology to include electric fields caused by surface ions, and ionic screening effects above the charged surfaces, in typical protein adsorption simulations. Using the adsorption of HEWL onto a negatively charged model silica surface as an exemplar, we have shown that the screening ions slow down the adsorption process, but fundamentally do not change the broad conclusions we draw from these simulations. The orientation of the adsorbed protein is determined by the alignment of its dipole moment with the electric field above the surface. Provided the protein has adequate time to rotate, the adsorption results in the HEWL orientation previously labelled 'side-on' or 'between'[15,28,30-31]. The screening ions help provide the necessary time for the protein to explore the surface energy landscape, so the adsorption is more controlled. The adsorption process is driven by fluctuations in the electric field above the surface caused by the thermal motion of the screening ions. Furthermore, the ions also help to stabilise the protein once adsorbed, suggesting that the HEWL will retain its biological function with its active cleft exposed to solution and therefore available for interactions with other species.

More broadly, we have shown the importance of correctly including the effects of electric fields and ionic screening to protein adsorption at charged material surfaces. Our methodology can be applied using freely available simulation tools, and is therefore applicable to a range of technologically important systems where bio-compatibility or surface functionalisation is crucial. It is becoming widely accepted that not only protein orientation at the surface, but also the extent to which proteins retain their secondary and tertiary structures[12], is key to the protein functionality once adsorbed. The steering effects of electric fields[14-16], coupled with the stabilisation provided by the screening ions[43], may prove to be crucial aspects in the future development of functional devices.

Acknowledgements

The simulations were performed on the EPSRC funded ARCHIE-WeSt High Performance Computer (www.archie-west.ac.uk); EPSRC grant no. EP/K000586/1. DJC was supported by a University of Strathclyde studentship.

Notes and references

1 N. Huebsch and D. Mooney, *Nature,* 2009, ***462***, 426-432.
2 W. Norde and A. C. I. Anusiem, *Colloids Surf.* 1992, **66**, 73-80.
3 M. van der Veen, M. C. Stuart and W. Norde, *Colloids Surf.* 2007, **54**, 136-142.
4 F. Evers, K. Shokuie, M. Paulus, C. Sternemann, C. Czeslik and M. Tolan, *Langmuir* 2008, **24**, 10216-10221.
5 K. P. Fears, B. Sivaraman, G. L. Powell, Y. Wu and R. A. Latour, *Langmuir* 2009, **25**, 9319-9327.
6 H. Hahl, F. Evers, S. Grandthyll, M. Paulus, C. Sternemann, P. Loskill, M. Lessel, A. K. Huseken, T. Brenner, M. Tolan and K. Jacobs, *Langmuir* 2012, **28**, 7747-7756.
7 B. Jachimska and A. Pajor, *Bioelectrochemistry* 2012, **87**, 138-146
8 A. G. Richter and I. Kuzmenko, *Langmuir* 2013, **29**, 5167-5180.
9 B. Bharti, J. Meissner, S. H. L. Klapp and G. H. Findenegg, *Soft Matter* 2014, **10**, 718-728.
10 K. Xu, M. M. Ouberai and M. E. Welland, *Biomaterials*, 2013, **34**, 1461-1470.
11 M. Kastantin, B. B. Langdon and D. K. Schwartz, *Adv. Colloid Interface Sci.* 2014, **207**, 240-252.
12 A. A. Thyparambil, Y. Wei and R. A. Latour, *Biointerphases* 2015, **10**, 019002.
13 N. Hildebrand, S. Koppen, L. Derr, K. Li, M. Koleini, K. Rezwan and L. C. Ciacchi, J. *Phys. Chem. C* 2015, **119**, 7295-7307.
14 Y. Xie, C. Liao, and J. Zhou, *Biophys. Chem.* 2013, **179**, 26-34.
15 K. Kubiak-Ossowska, M. Cwieka, A. Kaczynska, B. Jachimska and P. A. Mulheran, *Phys. Chem. Chem. Phys.* 2015, **17**, 24070-24077.
16 K. Kubiak-Ossowska, P. A. Mulheran and W. Nowak, *Phys. Chem. B,* 2014, **118**, 9900-9908.

17 P. A. Mulheran, D. Pellenc, R. A. Bennett, R. J. Green and M. Sperrin, *Phys. Rev. Lett.* 2008, **100**, 068102.
18 D. Pellenc, R. A. Bennett, R. J. Green, M. Sperrin and P. A. Mulheran, *Langmuir* 2008, **24**, 9648-9655.
19 T. J. Su, J. R. Lu, R. K. Thomas, Z. F. Cui and J. Penfold, *J. Colloid Int. Sci.* 1998, **203**, 419-429.
20 S. M. Daly, T. M. Przybycien and R. D. Tilton, *Langmuir* 2003, **19**, 3848-3857.
21 J. R. Lu, M. J. Swann, L. L. Peel and N. J. Freeman, *Langmuir* 2004, **20**, 1827-1832
22 M. van der Veen, W. Norde and M. C. Stuart, *Colloids Surf.* 2004, **35**, 33-40.
23 S. Z. Qiao, H. Djojoputro, Q. Hu and G. Q. Lu, *Prog. Solid State Chem.* 2006, **34**, 249-256.
24 S. M. Daly, T. M. Przybycien and R. D. Tilton, *Colloids Surf. B* 2007, **57**, 81-88.
25 F. Dismer and J. A. Hubbuch, *J. Chromatogr. A* 2007, **1149**, 312-320.
26 F. Felsovalyi, P. Mangiagalli, Ch. Bureau, S. K. Kumar and S. Banta, *Langmuir* 2011, **27**, 11873-11882.
27 P. A. Mulheran and K. Kubiak, *Mol. Sim.* 2009, **35**, 561-566.
28 K. Kubiak, and P. A. Mulheran, *J. Phys. Chem. B* 2009, **113**, 12189-12200.
29 K. Kubiak–Ossowska and P. A. Mulheran, *Langmuir,* 2010, ***26***, 7690-7694.
30 K. Kubiak–Ossowska and P. A. Mulheran, *Langmuir,* 2010, ***26***, 15954-15965.
31 K. Kubiak–Ossowska and P. A. Mulheran, *J. Phys. Chem. B,* 2011, **115**, 8891-8900.
32 K. Kubiak-Ossowska and P. A. Mulheran, *Langmuir* 2012**, 28**, 15577-15585.
33 A. Steudle and J. Pleiss, *Biophys. J.* 2011, **100**, 3016-3024.
34 C. Mathe, S. Devineau, J. C. Aude, G. Lagniel, S. Chedin, V. Legros, M. H. Mathon, J. P. Renault, S. Pin, Y. Boulard and J. Labarre, *PLoS ONE* 2014, **8**, e81346.
35 K. Kubiak–Ossowska, G. Burley, S. V. Patwardhan and P. A. Mulheran, *J. Phys. Chem. B* 2013, **117**, 14666-14675.
36 S. V. Patwardhan, F. S. Emami, R. J. Berry, S. E. Jones, R. R. Naik, O. Deschaume, H. Heinz and C. C. Perry, *J. Am. Chem. Soc.* 2012, **134**, 6244-6256.
37 W. Friedrichs, S. Koppen and W. Langel, *Surf. Sci.* 2013 **617,** 42-52.
38 J. C. Phillips, R. Braun, W. Wang, J. Gumbart, E. Tajkhorshid, E. Villa, Ch. Chipot, R.D. Skeel, L. Kale and K. Schulten, *J. Comput. Chem.* 2005, **26**, 1781-1802.
39 U. Essmann, L. Perera, M. L. Berkowitz, T. Darden, H. Lee and L. A. Pederson, *J. Chem. Phys.* 1995, **103**, 8577-8593.
40 A.A. Skelton, P.Fenter, J.D. Kubicki, D.J. Wesolowski and P.T. Cummings, *J. Phys. Chem. C* 2011, **115**, 2076-2088.
41 W. Humphrey, A. Dalke and K. Schulten, *J. Molec. Graphics* 1996, **14**, 33-38.
42 C. Sauter, F. Otalora, J. A. Gavira, O. Vidal, R. Giege and J. M. Garcia-Ruiz, *Acta Crystallogr. D* 2001**, 57**, 1119-1126.
43 A. S. Parmar and M. Muschol, *Biophys J.* 2009, **97**, 590-598.

